



Cite this: *Org. Biomol. Chem.*, 2017, **15**, 4579

## Non-pericyclic cycloaddition of *gem*-difluorosubstituted azomethine ylides to the C=O bond: computational study and synthesis of fluorinated oxazole derivatives†

Karina R. Gaisina, Alexander F. Khlebnikov \* and Mikhail S. Novikov 

The cycloaddition of arenecarbaldehydes and  $\alpha,\alpha,\alpha$ -trifluoroacetophenones with *gem*-difluoro-substituted azomethine ylides, generated from *N*-benzhydrylideneamines and difluorocarbene, occurs regioselectively to give, after hydrolysis, oxazolidin-4-ones. The primary cycloadducts of trifluoroacetophenones, 4,4-difluoro-5-trifluoromethyloxazolidine derivatives, are sufficiently stable to be isolated in reasonable to excellent yields. The results of correlation analysis and DFT calculations reveal a non-pericyclic step-wise mechanism of the reaction. The replacement of the two geminal hydrogen atoms in the azomethine ylide intermediate for fluorine atoms results in a dramatic change in the reaction mechanism from pericyclic to step-wise, proceeding *via* a zwitterion-like transition state in which no C–O bonding is observed.

Received 1st March 2017,  
Accepted 4th May 2017

DOI: 10.1039/c7ob00521k

rsc.li/obc

### Introduction

The 1,3-dipolar cycloaddition of nitrogen ylides to carbon-heteroatom multiple bonds is an attractive synthetic approach to a great variety of five-membered heterocycles.<sup>1</sup> This strategy has usually the advantage of synthetic efficiency, and high regio- and stereoselectivities. The main features of this type of pericyclic reaction were formulated by Huisgen.<sup>1a,2</sup> Stereoselectivity and stereospecificity of the cycloaddition of nitrogen ylides to multiple bonds is typical of the reactions proceeding *via* a concerted pericyclic mechanism.<sup>1–3</sup> This mechanism is usually characteristic of reactions of azomethine ylides with multiple carbon–carbon bonds.<sup>1,2</sup> A switch from a concerted to a non-concerted pathway can, however, occur in the presence of certain combinations of substituents. Thus, strong electron-withdrawing substituents in dipolarophiles, like in dialkyl dicyanobutenedioates, can significantly reduce the barrier for the formation of zwitterionic intermediates in the reaction with azomethine ylides so that a stepwise cycloaddition can become competitive with a concerted cycloaddition.<sup>4</sup> At the same time, substituents in the azomethine

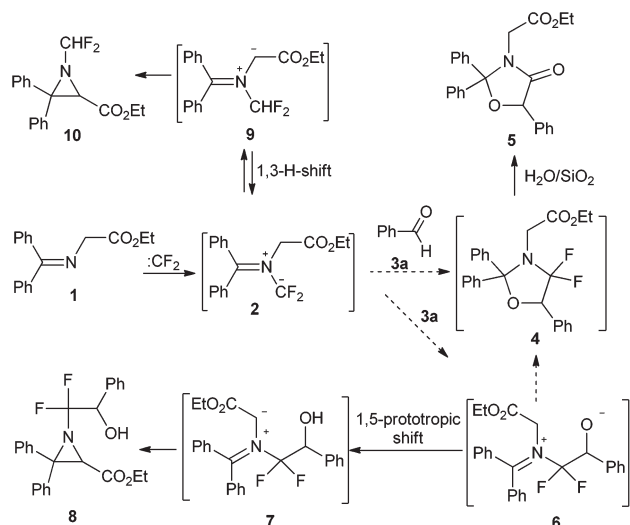
ylide, that destabilize the positive charge in the intermediate zwitterion, favour the concerted cycloaddition, even with C=C dipolarophiles with strong electron-withdrawing substituents.<sup>4b</sup> Because of the importance of fluorinated heterocycles in medicinal chemistry the cycloaddition of azomethine ylides and dipolarophiles containing fluorine atoms attracts a lot of attention.<sup>5</sup> The introduction of a fluorine atom, the most electronegative element, into a dipole or dipolarophile can have an influence on the mechanism of cycloaddition. Earlier it was found that the 1,3-dipolar cycloaddition of difluoro azomethine ylides to fumaronitrile and maleonitrile is stereoselective, consistent with a concerted mechanism for the reaction.<sup>6</sup>

The cycloaddition of iminodifluoromethanides to the C=O double bond of aldehydes and ketones proceeds regioselectively but nonstereoselectively to give the corresponding oxazolidinones after hydrolysis of the unstable intermediate difluorooxazolidines.<sup>7</sup> The reaction of azomethine ylide **2**, generated from ethyl benzhydrylidene glycinate **1**, proceeds in a more complex manner providing aziridines **8** and **10** along with the expected oxazolidinone **5** (Scheme 1). Aziridine **10** is the product of ylide **2**–ylide **9** isomerization followed by 1,3-cyclization.<sup>8</sup> The formation of aziridine **8** can proceed *via* zwitterion **6**, resulting from the nucleophilic addition of ylide **2**, to the carbonyl carbon of benzaldehyde, followed by a 1,5-prototropic shift to give ylide **7**, which then undergoes a 1,3-cyclization. This implies that the formation of oxazolidine **4** can be the result of a nonconcerted cycloaddition of the fluorinated ylide to the C=O double bond of benzaldehyde.

St. Petersburg State University, Institute of Chemistry, 7/9 Universitetskaya nab., St. Petersburg, 199034 Russia. E-mail: a.khlebnikov@spbu.ru; Fax: +7 812-428-6939; Tel: +7 812-428-9344

† Electronic supplementary information (ESI) available: Spectroscopic data for all new compounds, competition reaction experiments and computational details. See DOI: 10.1039/c7ob00521k





Scheme 1 Reaction of fluorinated ylide 2 with benzaldehyde.<sup>7</sup>

## Results and discussion

To shed some light on the mechanism of the reaction of iminodifluoromethanides with carbonyl compounds we turned to the correlation analysis and the quantum-chemical calculations for cycloadditions of iminodifluoromethanides 2 and 12 with arenecarbaldehydes. The information on the structure of the transition state of the cycloaddition of *gem*-difluorinated ylide can be retrieved from the  $\rho$  value of the Hammett equation for reactions of a series of arenecarbaldehydes with ylide 12 derived from imine 11 and difluorocarbenes. We carried out the reactions of imine 11 with *para*-substituted benzaldehydes 3a–e in the presence of a difluorocarbene source. Heating a mixture of amine 11, aldehyde, dibromodifluoromethane, lead filings and  $\text{Bu}_4\text{NBr}$  in dichloromethane at 40 °C under ultrasound irradiation gave a mixture containing difluorooxazolidines 13. Due to the fast hydrolysis of compounds 13 during the work-up of the reaction mixture, the difluorooxazolidines could not be isolated. Instead oxazolidinones 14a–e were isolated by column chromatography in 52–73% yield (Table 1).

The obtained relative reaction constants from Hammett competition reaction experiments for aldehydes 3a–e are listed in Table 2 (for details see the ESI†) and were used for a Hammett correlation with  $\sigma$ -constants. A plot of Hammett  $\sigma$ -values vs.  $\log k_{\text{R}}/k_{\text{H}}$  for reactions of aldehydes 3a–e gave a satisfactory linear correlation:  $\log k_{\text{R}}/k_{\text{H}} = \rho\sigma = (0.08 \pm 0.05) + (1.56 \pm 0.14)\sigma$  ( $R = 0.988$ ,  $\text{SD} = 0.105$ ,  $N = 5$ ).

A positive  $\rho$  value in the Hammett equation indicates an increase of electron density on the carbon atom of the dipolarophile in the transition state. It can occur either within a step-wise mechanism of the reaction involving a zwitterionic intermediate of type 6 or within an asynchronous concerted cycloaddition in which the C–C bond is formed ahead of the C–O bond. Analysis of the  $\rho$  value in the Hammett equation may be based on a comparison with the corresponding constants of

Table 1 Synthesis of oxazolidine 14a–e

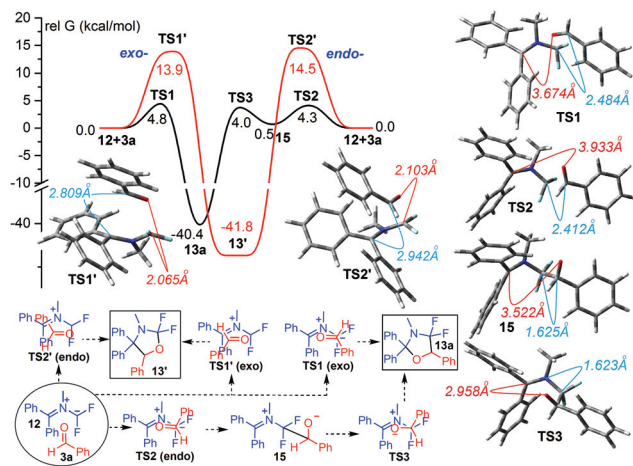
Entry	Ar	3	14, yield, %
1	Ph	a	a, 64
2	4-MeC <sub>6</sub> H <sub>4</sub>	b	b, 52
3	4-MeOC <sub>6</sub> H <sub>4</sub>	c	c, 70
4	4-ClC <sub>6</sub> H <sub>4</sub>	d	d, 73
5	4-NCC <sub>6</sub> H <sub>4</sub>	e	e, 72

Table 2 The relative constants for the reactions of aldehydes 3a–e with azomethine ylide 12 in dichloromethane (DCM) at 40 °C and  $\sigma$ -constants used for Hammett correlation<sup>9</sup>

Entry	Ar	3	$k_{\text{R}}/k_{\text{H}} \pm s_{\text{m}}$	$\sigma$
1	4-MeOC <sub>6</sub> H <sub>4</sub>	c	$0.235 \pm 0.003$	–0.27
2	4-MeC <sub>6</sub> H <sub>4</sub>	b	$0.481 \pm 0.029$	–0.17
3	Ph	a	1.0	0
4	4-ClC <sub>6</sub> H <sub>4</sub>	d	$2.23 \pm 0.15$	0.23
5	4-NCC <sub>6</sub> H <sub>4</sub>	e	$7.56 \pm 0.75$	0.66

related reaction series. Unfortunately, not so many studies deal with a Hammett analysis of the interaction of ylides with benzaldehydes, and such information related to the reaction of nitrogen ylides is absent in the literature. Some data were published for the Wittig reaction of substituted benzaldehydes with alkylidene-triphenylphosphoranes, for which the corresponding correlation with the  $\sigma$ -values gives a positive  $\rho$  value in the range 0.2–3.2.<sup>10</sup> A positive  $\rho$  value, 1.6–2.1, in the corresponding Hammett equations was found for Wittig–Horner reactions of phosphonates and substituted benzaldehydes.<sup>11</sup> Substituent effects on the reaction rate of the epoxidation of benzaldehydes with sulfur ylides, proceeding *via* a zwitterionic transition state, were studied, and a Hammett  $\rho$  of +2.50 was found.<sup>12</sup> This means that data from relative rates and Hammett correlation are not enough to make a conclusion about the mechanism of the cycloaddition. Calculations of transition states of the reactions of ylide 12 with benzaldehydes 3 and ylide 16 with benzaldehyde 3a at the DFT B3LYP/6-31G(d) level<sup>13</sup> using the PCM solvent model<sup>14</sup> were therefore performed. There are four possible ways ylide 12 can approach the carbonyl group of benzaldehyde 3a (Fig. 1). The first two approaches involve the formation of the C–C bond between the carbonyl carbon and  $\text{CF}_2$ -group and lead to the formation of oxazolidine 13: (1) H of the formyl group *syn*-oriented to the N–Me bond of the ylide (*exo*-approach, **TS1**)





**Fig. 1** Energy profiles for the reactions of benzaldehyde **3a** with fluorinated ylide **12**. Relative free Gibbs energies (in kcal mol<sup>-1</sup>, 298 K, PCM model for DCM) computed at the DFT B3LYP/6-31G(d) level.

and (2) H of the formyl group *anti*-oriented to the N-Me bond of the ylide (*endo*-approach, **TS2**). The second two approaches involve the formation of the C-C bond between the carbonyl carbon and CPh<sub>2</sub>-group and lead to the formation of oxazolidine **13'**: (3) H of the formyl group *syn*-oriented to the N-Me bond of the ylide (*exo*-approach, **TS1'**) and (4) H of the formyl group *anti*-oriented to the N-Me bond of the ylide (*endo*-approach, **TS2'**).

According to the calculations the energies of **TS1'** and **TS2'** are much higher than the energies of **TS1** and **TS2**. This ensures the regioselectivity of the reaction with the formation of oxazolidine **13a** as a sole product. The pathway (1) leads directly to the difluorooxazolidine **13** via the transition state **TS1**, and although formation of the new bonds is quite asynchronous (F<sub>2</sub>C-C=O distance is 2.484 Å and Ph<sub>2</sub>C-O distance is 3.674 Å for the reaction of **3a**) it is impossible to locate any minimum on the energy surface that could correspond to a zwitterion. In contrast, the pathway (2) leads via the transition state **TS2** (CF<sub>2</sub>-C=O distance is 2.412 Å and Ph<sub>2</sub>C-O distance is 3.933 Å) to zwitterion **15** (CF<sub>2</sub>-C=O distance is 1.625 Å and Ph<sub>2</sub>C-O distance is 3.522 Å), and then to difluorooxazolidine **13a** via the transition state **TS3** (F<sub>2</sub>C-C=O distance is 1.623 Å and Ph<sub>2</sub>C-O distance is 2.958 Å) (Fig. 1). This means that the pathway (1) gives a cycloaddition product as a result of a concerted, non-pericyclic very asynchronous process, whereas the pathway (2) by a step-wise cycloaddition with the formation of a zwitterionic intermediate.

The calculations, using dispersion-inclusive functional wB97XD<sup>15</sup> and the MPWB1K functional<sup>16</sup> together with the 6-311G(d,p) basis set, which was recently used for study of the [3 + 2] cycloaddition reaction of nitrones with ketenes,<sup>17</sup> were additionally performed for the reaction of ylide **12** with benzaldehyde **3a** in order to instill confidence in the calculation results (Fig. 2). The results obtained show that the change in the functional and the basis set has little effect on the relative

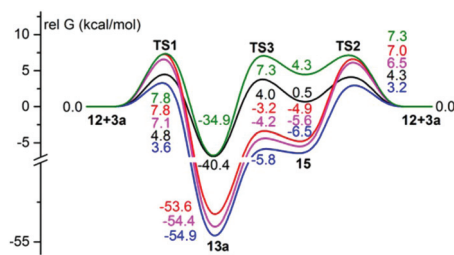


**Fig. 2** Energy profiles for the reaction of ylide **12** and benzaldehyde **3a**. Relative free Gibbs energies (in kcal mol<sup>-1</sup>, 298 K, PCM model for DCM) computed: black – optimization of geometry at the DFT B3LYP/6-31G(d) level; green – single point calculation at the DFT B3LYP/6-311G(d,p) level with B3LYP/6-31G(d) optimized geometries; red – single point calculation at the DFT MPWB1K/6-311G(d,p) level with B3LYP/6-31G(d) optimized geometries; magenta – optimization of geometry at the DFT MPWB1K/6-311G(d,p) level; blue – single point calculation at the DFT wB97XD/6-311G(d,p) level with B3LYP/6-31G(d) optimized geometries.

energies of the transition states **TS1** and **TS2**, and thus does not affect the conclusions made.

Nevertheless, for all energy profiles presented in Fig. 3–5, in addition to the calculations performed at the DFT B3LYP/6-31G(d) level of theory, the single point calculations were also made at the wB97XD/6-311G(d,p) and MPWB1K/6-311G(d,p) levels with B3LYP/6-31G(d) optimized geometries. A comparison of the experimental relative rate constants of the reactions of the ylide **12** and substituted benzaldehydes **3a–e** with the corresponding relative free Gibbs energies of the transition states of **TS2** showed that the best correlation is observed for energies obtained at the B3LYP/6-31G(d) level:  $\Delta G^\ddagger = 6.6 \pm 0.2 - (2.3 \pm 0.3) \lg k_R/k_H$  [ $R = 0.925$ ,  $SD = 0.391$ ,  $N = 5$ ; single point calculations at the MPWB1K/6-311G(d,p) level with B3LYP/6-31G(d) optimized geometries];  $\Delta G^\ddagger = 3.0 \pm 0.1 - (2.5 \pm 0.3) \lg k_R/k_H$  [ $R = 0.954$ ,  $SD = 0.279$ ,  $N = 5$ ; single point calculations at the wB97XD/6-311G(d,p) level with B3LYP/6-31G(d) optimized geometries];  $\Delta G^\ddagger = 4.4 \pm 0.1 - (2.4 \pm 0.2) \lg k_R/k_H$

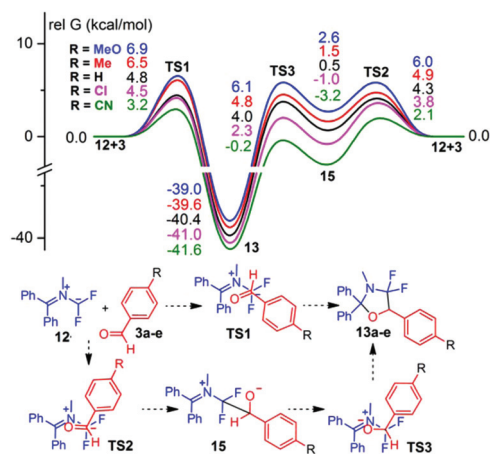


**Fig. 3** Energy profiles for the reaction of ylide **12** and benzaldehydes **3a–e**. Relative free Gibbs energies (in kcal mol<sup>-1</sup>, 298 K, PCM model for DCM) computed at the DFT B3LYP/6-31G(d).



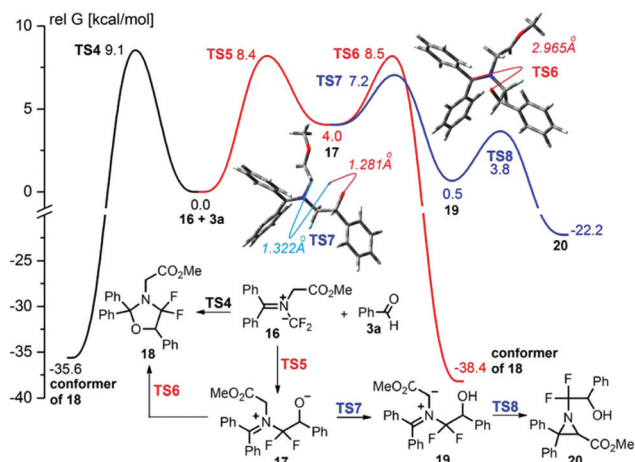


**Fig. 4** Energy profiles for the transformations of **16**. Relative free Gibbs energies (in kcal mol<sup>-1</sup>, 298 K, PCM model for DCM) computed at the DFT B3LYP/6-31G(d) level.

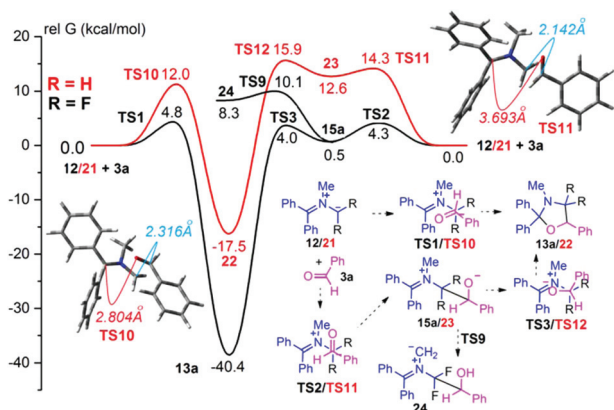


**Fig. 5** Energy profiles for the reactions of benzaldehyde **3a** with fluorinated ylide **12** and non-fluorinated ylide **21**. Relative free Gibbs energies (in kcal mol<sup>-1</sup>, 298 K, PCM model for DCM) computed at the DFT B3LYP/6-31G(d) level.

[ $R = 0.976$ ,  $SD = 0.191$ ,  $N = 5$ ; at the B3LYP/6-31G(d) level]. The calculation results obtained at the B3LYP/6-31G(d) level are presented, therefore, in Fig. 3–5, whereas the results obtained at other levels can be found in Fig. S3–S5 (ESI).<sup>†</sup>

The free Gibbs energies of both transition states of the step-wise mechanism (TS2 by 0.5–1.6 kcal mol<sup>-1</sup> and TS3 by 0.8–3.0 kcal mol<sup>-1</sup>) are lower than the energies of the transition state (TS1) for a concerted mechanism for all substituted benzaldehydes **3a–e**. The formation of the product therefore proceeds mostly *via* the zwitterionic intermediate. In accordance with the experimental data the electron-withdrawing substituents in the benzene ring of aldehydes **3a–e** reduce the barriers for addition of the ylide **12** to the C=O bond, while the donating substituents increase them.

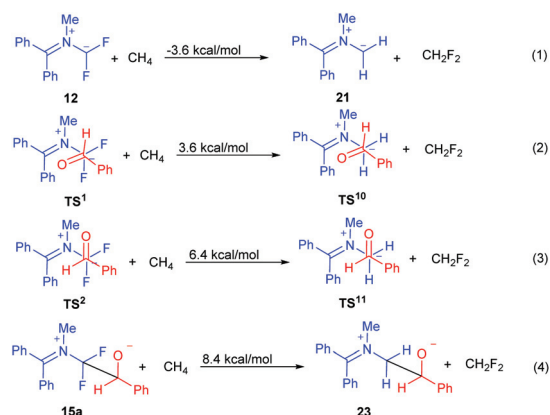
These data assume that the formation of a complex mixture of products for the reaction of ylide **2** with benzaldehyde could really be a result of the non-concertedness of the cycloaddition

of the fluorinated ylide to the C=O bond (Scheme 1). To evaluate the relative energies of the transition states of the reaction leading to products **5** and **8** we performed DFT calculations of the transformations of the nearest analogue of **2**, the corresponding methyl ester **16** (Fig. 4).

According to the calculation, the barrier for a concerted cycloaddition of ylide **16** to the C=O bond of benzaldehyde **3a** is higher by 0.7 kcal mol<sup>-1</sup> than the barrier for the formation of the zwitterion **17**, the intermediate of the step-wise route to oxazolidine **18**. It is noteworthy that the barrier for the 1,5-prototropic shift in the zwitterion leading to ylide **19**, the isomer of starting ylide **16**, is lower than the barrier for cyclization of the zwitterion to oxazolidine **18** by 1.3 kcal mol<sup>-1</sup>. This means that the formation of aziridine **20** can indeed compete with the formation of oxazolidine **18** due to the preference of the step-wise addition of the ylide **16** to the C=O bond. Such a low barrier for the transformation of zwitterion **17** into ylide **19** (3.2 kcal mol<sup>-1</sup>) is largely due to the influence of the electron-withdrawing alkoxy carbonyl group.

In fact, the barrier for the transformation of zwitterion **15a** without such an activating group into the corresponding ylide **24** is much higher (TS9, 10.1 kcal mol<sup>-1</sup>) and that, together with the low barrier for cyclization of **15a** (TS3), is preventing the formation of the corresponding aziridine in this case (Fig. 5).

In order to evaluate how the introduction of fluorine atoms into the ylidic carbon effects the concertedness of the cycloaddition to the C=O bond the calculation of the interaction of non-fluorinated ylide **21** with benzaldehyde **3a** was performed (Fig. 5). According to calculations the concerted cycloaddition (TS10) is, in this case, much more preferred than the step-wise one (TS11, TS12). Moreover, the formation of C–C and C–O bonds becomes more synchronous (F<sub>2</sub>C–C=O distance is 2.484 Å and Ph<sub>2</sub>C–O distance is 3.674 Å (TS1); H<sub>2</sub>C–C=O distance is 2.316 Å and Ph<sub>2</sub>C–O distance is 2.804 Å (TS10)). Analysis of the isodesmic equations shows that the replacement of both fluorine atoms in ylide **12** with hydrogens (ylide **21**) leads to the stabilization of the ylide species (Scheme 2,



**Scheme 2** The isodesmic equations for ylides **12/21**, zwitterions **15a/23** and transition states **TS1/TS10** and **TS2/TS11**. Relative free Gibbs energies (in kcal mol<sup>-1</sup>, 298 K, PCM model for DCM) computed at the DFT B3LYP/6-31G(d) level.



reaction (1)). This can be explained by the strong pyramidalization of the NCF<sub>2</sub> moiety (pyramidalization angle in ylide **12** is 21.3° versus 1.8° for ylide **21**), resulting in the decrease of conjugation in the π-system of the fluorinated 1,3-dipole.

The destabilizing effect of fluorine atoms vanishes in transition state **TS1** and becomes a stabilizing effect in **TS2** and even more in zwitterion **15a**. Thus, the strong pyramidalization of the NCF<sub>2</sub> moiety of ylide **12**, most probably, is the main cause of the two-stage mechanism of the cycloaddition.

As mentioned above, fluorinated oxazolidines **13** very easily undergo hydrolysis, losing fluorine. As fluorinated heterocycles are widely used as drugs, agrochemicals and materials with special properties<sup>18</sup> it would be useful to use the reaction described above to prepare fluorinated derivatives of oxazolidine of type **13**. Some perfluorinated oxazolidines have been prepared by the electrochemical fluorination of derivatives of aminosubstituted carboxylic acids in low yield.<sup>19</sup> The intramolecular cycloaddition of difluorinated azomethine ylides to an ester carbonyl group gives heterocycles with difluorinated oxazolidine as a part of the bridged system.<sup>1c,20</sup> Analysis of these data allows us to conclude that strong electron-withdrawing substituents, like the CF<sub>3</sub>-group, and a substitution pattern which prevents dehydrofluorination, will stabilise the fluorinated oxazolidine. Taking into account the above results, showing that electron-withdrawing substituents accelerate the reaction of fluorinated ylides with a carbonyl group, we decided that CF<sub>3</sub>-substituted ketones are good starting materials for the preparation of oxazolidines with fluoro- and trifluoromethyl-substituents. The experimental results confirmed the correctness of our assumptions: 4,4-difluoro-5-trifluoromethyl-substituted oxazolidines were obtained in synthetically significant yields (Table 3). The oxazolidines **28** were, however, still acid sensitive, therefore to preserve fluorine at the ring the isolation of the products should be performed

without chromatography on silica. The addition of a catalytic amount of HCl to the DCM solution of the oxazolidines **28** leads to their quantitative transformation into the corresponding oxazolidinones **29** (Table 3).

It is notable that the formation of aziridine **10** in the reaction of imine **1** with trifluoroacetophenone under difluorocarbene generation conditions was not observed. This fact can be explained by the higher electrophilicity of trifluoroacetophenone compared with benzaldehyde, resulting in the inhibition of the isomerization of ylide **2** to ylide **9**. The second competing pathway of the reaction, a 1,5-prototropic shift in the zwitterionic intermediate leading to an aziridine product of type **8**, is not realized as well. This is probably due to the reduced basicity of theolate oxygen of the corresponding CF<sub>3</sub>-substituted zwitterionic intermediate which results in an increase of the barrier for the 1,5-prototropic shift.

## Conclusions

We have shown that the cycloaddition of arenecarbaldehydes with *gem*-difluoro-substituted azomethine ylides, generated from benzhydrylidene amines and difluorocarbenes, occurs regioselectively to give after hydrolysis oxazolidin-4-ones. The change of a benzaldehyde for an α,α-trifluoroacetophenone as a dipolarophilic agent results in (a) an increase of the stability of the primary difluoropyrrolidine cycloadduct, and (b) inhibition of the competing 1,5-prototropic shift in the zwitterion intermediate. This allowed the isolation of 4,4-difluoro-5-trifluoromethylpyrrolidine cycloadducts in reasonable to excellent yields. Correlation analysis and DFT calculations reveal a non-pericyclic step-wise mechanism of the reaction. The exchange of the two geminal hydrogen atoms in an azomethine ylide intermediate with fluorines results in a dramatic change in the reaction mechanism from pericyclic to step-wise, *via* a zwitterion-like transition state, in which no C–O bonding is observed.

## Experimental

### General

Melting points were determined on a hot stage microscope and are uncorrected. <sup>1</sup>H (300 MHz, 400 MHz) and <sup>13</sup>C (75 MHz, 100 MHz) NMR spectra were determined in CDCl<sub>3</sub> with a Bruker DPX 300 and a Bruker AVANCE III 400. Chemical shifts (δ) are reported in parts per million downfield from tetramethylsilane (TMS δ = 0.00); <sup>1</sup>H NMR spectra were calibrated according to the residual peak of CDCl<sub>3</sub> (<sup>1</sup>H 7.26 ppm, <sup>13</sup>C 77.00 ppm). <sup>19</sup>F NMR spectra were recorded at 376 MHz; chemical shifts are reported in ppm from CFCl<sub>3</sub> as an internal standard. Elemental analysis was performed on a Hewlett-Packard 185B CHN-analyser. Silica gel Merck 60 was used for column chromatography. Thin-layer chromatography (TLC) was conducted on alumina sheets precoated with SiO<sub>2</sub> ALUGRAM SIL G/UV254.

**Table 3** Synthesis of oxazolidines **28a–d** and oxazolidinones **29a–d**

Entry	R <sup>1</sup>	R <sup>2</sup>	Imine	27	28, yield, %	29, yield, %
1	Me	Ph	<b>11</b>	<b>a</b>	<b>a</b> , 63	<b>a</b> , 89 <sup>a</sup>
2	Me	4-MeC <sub>6</sub> H <sub>4</sub>	<b>11</b>	<b>b</b>	<b>b</b> , 64	—
3	Me	4-ClC <sub>6</sub> H <sub>4</sub>	<b>11</b>	<b>c</b>	—	<b>b</b> , 55 <sup>a</sup>
4	Bn	Ph	<b>25a</b>	<b>a</b>	<b>c</b> , 58	<b>c</b> , 95 <sup>a</sup>
5	CH <sub>2</sub> CO <sub>2</sub> Et	Ph	<b>1</b>	<b>a</b>	<b>d</b> , 90	—
6	Me	Bn	<b>11</b>	<b>d</b>	—	<b>d</b> , 60 <sup>b</sup>

<sup>a</sup> After hydrolysis of **28**. <sup>b</sup> Chromatography on silica.



## Calculation details

All calculations were performed with the density functional method by using the Gaussian 09 suite of programs. Geometry optimizations of intermediates, transition states,<sup>21</sup> reactants, and products in dichloromethane were performed at the DFT B3LYP/6-31G(d) level<sup>13</sup> using the PCM solvent model.<sup>14</sup> Stationary points on the respective potential-energy surfaces were characterized at the same level of theory by evaluating the corresponding Hessian indices. Careful verification of the unique imaginary frequencies for transition states was carried out to check whether the frequency indeed pertains to the desired reaction coordinate. Single-point calculations with B3LYP/6-31G(d) optimized geometries, using dispersion-inclusive functional wB97XD<sup>15</sup> and the MPWB1K<sup>16</sup> functional together with the 6-311G(d,p) basis set were additionally performed.

**A typical experimental procedure for the synthesis of oxazolidinones 14a–e.** A flask containing freshly prepared lead filings (2.08 g, 10 mmol) and dry dichloromethane (25 mL) was charged with Bu<sub>4</sub>NBr (6.45 g, 20 mmol), *N*-benzhydrylidene-*N*-methylamine **11** (5 mmol), aldehyde (10 mmol) and CF<sub>2</sub>Br<sub>2</sub> (4.20 g, 20 mmol). The flask was tightly stoppered, immersed in an ultrasonic cleaner (160 W) and irradiated with ultrasound at 40 °C until the lead was completely consumed (5–10 h). The solvent was removed under reduced pressure, and the residue was separated by column chromatography on silica to afford oxazolidinones **14a–e**. Crystalline products were recrystallised from a mixture of hexane–Et<sub>2</sub>O.

**3-Methyl-2,2,5-triphenyloxazolidin-4-one (14a).** Colourless solid; m.p. 106–108 °C (Et<sub>2</sub>O/hexane); δ<sub>H</sub> (300 MHz, CDCl<sub>3</sub>) 2.89 (3H, s), 5.34 (1H, s), 7.36–7.47 (15H, m); δ<sub>C</sub> (75 MHz, CDCl<sub>3</sub>) 28.0, 78.4, 97.9, 127.1, 127.3, 128.2, 128.3, 128.4, 128.5, 129.0, 129.2, 135.8, 139.36, 139.39, 170.3. Anal. calcd for C<sub>22</sub>H<sub>19</sub>NO<sub>2</sub>: C, 80.22; H 5.81; N 4.25. Found: C, 80.12; H, 5.77; N, 4.23.

**3-Methyl-2,2-diphenyl-5-(*p*-tolyl)oxazolidin-4-one (14b).** Colourless solid; m.p. 81–83 °C (Et<sub>2</sub>O/hexane); δ<sub>H</sub> (300 MHz, CDCl<sub>3</sub>) 2.36 (3H, s), 2.87 (3H, s), 5.28 (1H, s), 7.19–7.21 (2H, m), 7.34–7.44 (12H, m); δ<sub>C</sub> (75 MHz, CDCl<sub>3</sub>) 21.2, 28.0, 78.4, 97.7, 127.2, 127.3, 128.2, 128.3, 128.4, 129.0, 129.2, 132.8, 138.3, 139.4, 139.5, 139.2, 170.5. Anal. calcd for C<sub>23</sub>H<sub>21</sub>NO<sub>2</sub>: C, 80.44; H 6.16; N 4.08. Found: C, 80.39; H, 6.12; N, 4.01.

**5-(4-Methoxyphenyl)-3-methyl-2,2-diphenyloxazolidin-4-one (14c).** Colourless solid; m.p. 107–108 °C (Et<sub>2</sub>O/hexane); δ<sub>H</sub> (300 MHz, CDCl<sub>3</sub>) 2.88 (3H, s), 3.81 (3H, s), 5.26 (1H, s), 6.91–6.94 (2H, m), 7.35–7.47 (12H, m); δ<sub>C</sub> (75 MHz, CDCl<sub>3</sub>) 28.0, 55.3, 78.2, 97.6, 114.0, 127.3, 127.9, 128.2, 128.3, 128.4, 128.8, 120.0, 129.2, 139.4, 139.5, 159.9, 170.6. Anal. calcd for C<sub>23</sub>H<sub>21</sub>NO<sub>3</sub>: C, 76.86; H 5.89; N 3.90. Found: C, 76.69; H 5.90; N 3.90.

**5-(4-Chlorophenyl)-3-methyl-2,2-diphenyloxazolidin-4-one (14d).** Colourless solid; m.p. 132–134 °C (Et<sub>2</sub>O/hexane); δ<sub>H</sub> (300 MHz, CDCl<sub>3</sub>) 2.87 (3H, s), 5.32 (1H, s), 7.33–7.46 (14H, m); δ<sub>C</sub> (75 MHz, CDCl<sub>3</sub>) 28.0, 77.6, 98.1, 127.3, 128.1, 128.2, 128.4, 128.5, 128.6, 129.1, 129.4, 134.3, 139.2, 139.3, 169.8. Anal.

calcd for C<sub>22</sub>H<sub>18</sub>ClNO<sub>2</sub>: C, 72.62; H 4.99; N 3.85. Found: C, 72.92; H 5.04; N 3.84.

**4-(3-Methyl-4-oxo-2,2-diphenyloxazolidin-5-yl)benzotrile (14e).** Colourless solid; m.p. 111–112 °C (Et<sub>2</sub>O/hexane); δ<sub>H</sub> (300 MHz, CDCl<sub>3</sub>) 2.85 (3H, s), 5.41 (1H, s), 7.32–7.35 (2H, m), 7.39–7.49 (8H, m), 7.56–7.59 (2H, m), 7.63–7.66 (2H, m); δ<sub>C</sub> (75 MHz, CDCl<sub>3</sub>) 28.1, 77.3, 98.4, 112.0, 118.5, 126.9, 127.3, 128.48, 128.50, 129.3, 129.5, 132.1, 138.8, 139.1, 141.0, 169.0. Anal. calcd for C<sub>23</sub>H<sub>18</sub>N<sub>2</sub>O<sub>2</sub>: C, 77.95; H 5.12; N 7.90. Found: C, 78.06; H 5.17; N 7.97.

**Synthesis of CF<sub>3</sub>-substituted oxazolidines 28a–d and oxazolidinones 29a–d.** Oxazolidines **28a–d** were prepared according to the method described above except for the work-up procedure. The reaction mixture was filtered, the filter-cake was washed with dichloromethane, and the filtrate was washed with 2% aq. Na<sub>2</sub>SO<sub>4</sub>. The solvent was evaporated on a rotary evaporator and the residue was recrystallised from a mixture of hexane–Et<sub>2</sub>O to give oxazolidines **28a–d**. Oxazolidinones **29a–d** were obtained from the corresponding oxazolidines **28a–d** by keeping their solutions at room temperature in wet dichloromethane containing traces of HCl for 2–10 days or by chromatography on silica.

**4,4-Difluoro-3-methyl-2,2,5-triphenyl-5-(trifluoromethyl)oxazolidine (28a).** Colourless solid; m.p. 102–103 °C (Et<sub>2</sub>O/hexane); δ<sub>H</sub> (300 MHz, CDCl<sub>3</sub>) 2.48 (3H, t, *J* 1.7 Hz), 7.11–7.14 (2H, m), 7.24–7.33 (3H, m), 7.43–7.48 (6H, m), 7.52–7.55 (2H, m), 7.70–7.73 (2H, m); δ<sub>C</sub> (75 MHz, CDCl<sub>3</sub>) 28.2 (dd, 4, 1 Hz), 85.5 (dq, *J* 30, 5 Hz), 101.5 (dd, *J* 5.2, 1.5 Hz), 122.5 (q, *J* 287 Hz), 124.0 (dd, *J* 245, 261 Hz), 127.5, 127.5, 127.8, 127.9, 128.5, 128.6, 128.7, 129.3, 131.1, 140.4 (d, *J* 4.5 Hz), 140.6 (d, *J* 3.6 Hz). Anal. calcd for C<sub>23</sub>H<sub>18</sub>F<sub>5</sub>NO: C, 65.87; H 4.33; N 3.34. Found: C, 65.70; H 4.42; N 3.25.

**4,4-Difluoro-3-methyl-2,2-diphenyl-5-(*p*-tolyl)-5-(trifluoromethyl)oxazolidine (28b).** Colourless solid; m.p. 104–105 °C (Et<sub>2</sub>O/hexane); δ<sub>H</sub> (300 MHz, CDCl<sub>3</sub>) 2.42 (3H, s), 2.45 (3H, t, *J* 1.7 Hz), 7.09–7.12 (2H, m), 7.24–7.29 (5H, m), 7.41–7.43 (2H, m), 7.49–7.52 (2H, m), 7.56–7.59 (2H, m); δ<sub>C</sub> (75 MHz, CDCl<sub>3</sub>) 21.2, 28.2 (dd, *J* 1.4, 4.4 Hz), 85.5 (dq, *J* 5, 30 Hz), 101.4 (dd, *J* 2, 5 Hz), 122.5 (q, *J* 287 Hz), 124.1 (dd, *J* 244, 261 Hz), 127.4, 127.67, 127.73, 128.1, 128.3, 128.5, 128.55, 128.61, 129.8, 130.21, 130.24, 139.2, 140.5 (d, 2.8 Hz) 140.6 (d, 4.5 Hz). Anal. calcd for C<sub>24</sub>H<sub>20</sub>F<sub>5</sub>NO: C, 66.51; H 4.65; N 3.23. Found: C, 66.40; H 4.68; N 3.12.

**3-Benzyl-4,4-difluoro-2,2,5-triphenyl-5-(trifluoromethyl)oxazolidine (28c).** Colourless solid; m.p. 120–121 °C (Et<sub>2</sub>O/hexane); δ<sub>H</sub> (300 MHz, CDCl<sub>3</sub>) 4.03 (1H, dd, *J* 1.7, 15.6 Hz), 4.12 (1H, dd, *J* 2.6, 15.6 Hz), 7.21–7.41 (16H, m), 7.61–7.63 (5H, m), 7.41–7.43 (4H, m); δ<sub>C</sub> (75 MHz, CDCl<sub>3</sub>) 47.3 (dd, *J* 2, 3 Hz), 85.7 (dq, *J* 5, 31 Hz), 102.3 (dd, *J* 1, 5 Hz), 122.6 (q, *J* 288 Hz), 124.5 (dd, *J* 247, 262 Hz), 127.0, 127.3, 127.5, 127.7, 127.8, 128.2, 128.3, 128.6, 128.73, 128.76, 128.82, 129.2, 130.9, 136.4, 140.8 (d, 4 Hz) 141.1 (d, 3 Hz). Anal. calcd for C<sub>29</sub>H<sub>22</sub>F<sub>5</sub>NO: C, 70.30; H 4.48; N 2.83. Found: C, 70.34; H 4.50; N 2.77.

**Ethyl 2-(4,4-difluoro-5-(trifluoromethyl)-2,2,5-triphenyloxazolidin-3-yl)acetate (28d).** Colourless solid; m.p. 85–86 °C (Et<sub>2</sub>O); δ<sub>H</sub> (400 MHz, CDCl<sub>3</sub>) 1.20 (3H, t, *J* 7.2 Hz), 3.60 (1H, dd, 2.0,



17.4 Hz), 3.72 (1H, dd, 2.9, 17.4 Hz), 3.99–4.14 (2H, m), 7.18–7.66 (15H, m);  $\delta_{\text{C}}$  (100 MHz,  $\text{CDCl}_3$ ) 13.8, 44.0, 61.2, 85.9 (dq,  $J$  7, 31 Hz), 101.6 (d,  $J$  3 Hz), 122.5 (q,  $^1J_{\text{CF}}$  288,  $\text{CF}_3$ ), 123.5 (dd,  $^1J_{\text{CF}}$  250; 259,  $\text{CF}_2$ ), 127.4, 127.7, 127.8, 127.9, 128.0, 128.3 (q,  $J$  7 Hz), 128.9, 129.0, 129.2, 130.0, 130.06, 135.5, 140.0 (d,  $J$  4 Hz), 140.9, 168.4.  $^{19}\text{F}$  NMR (376 MHz,  $\text{CDCl}_3$ )  $\delta_{\text{F}}$  -69.95 (d,  $J$  184 Hz), -71.36. Anal. calcd for  $\text{C}_{26}\text{H}_{22}\text{F}_5\text{NO}_3$ : C 63.54, H 4.51, N 2.85. Found: C, 63.40, H 4.54, N 2.64.

**3-Methyl-2,2,5-triphenyl-5-(trifluoromethyl)oxazolidin-4-one (29a).** Colourless solid; m.p. 168–169 °C ( $\text{Et}_2\text{O}$ /hexane);  $\delta_{\text{H}}$  (300 MHz,  $\text{CDCl}_3$ ) 2.85 (3H, s), 6.98–7.01 (2H, m), 7.11–7.28 (8H, m), 7.46–7.57 (7H, m), 7.52–7.55 (2H, m), 7.70–7.73 (2H, m);  $\delta_{\text{C}}$  (75 MHz,  $\text{CDCl}_3$ ) 28.3, 81.5 (q,  $J$  31 Hz), 98.7, 122.5 (q,  $J$  285 Hz), 126.7 (q, 1 Hz) 127.5, 127.6, 128.0, 128.1, 128.3, 128.9, 129.0, 129.5, 131.2, 138.1, 139.1, 164.9. Anal. calcd for  $\text{C}_{23}\text{H}_{18}\text{F}_3\text{NO}_2$ : C, 69.52; H 4.57; N 3.50. Found: C, 69.66; H 4.55; N 3.50.

**5-(4-Chlorophenyl)-3-methyl-2,2-diphenyl-5-(trifluoromethyl)oxazolidin-4-one (29b).** Colourless solid; m.p. 129–130 °C ( $\text{Et}_2\text{O}$ /hexane);  $\delta_{\text{H}}$  (300 MHz,  $\text{CDCl}_3$ ) 2.85 (3H, s), 6.99–7.01 (2H, m), 7.11–7.14 (2H, m), 7.18–7.23 (2H, m), 7.27–7.32 (1H, m), 7.46–7.55 (7H, m);  $\delta_{\text{C}}$  (75 MHz,  $\text{CDCl}_3$ ) 28.3, 81.1 (q,  $J$  31 Hz), 98.8, 122.3 (q,  $J$  285 Hz), 127.4, 127.9, 128.0, 120.0, 128.2, 128.3, 129.2, 129.6, 129.8, 135.2, 137.8, 139.0, 164.5. Anal. calcd for  $\text{C}_{23}\text{H}_{17}\text{ClF}_3\text{NO}_2$ : C, 63.97; H 3.97; N 3.24. Found: C, 63.95; H 4.06; N 3.24.

**Ethyl 2-(4-oxo-2,2,5-triphenyl-5-(trifluoromethyl)oxazolidin-3-yl)acetate (29c).** Colourless solid; m.p. 85–86 °C ( $\text{Et}_2\text{O}$ );  $\delta_{\text{H}}$  (400 MHz,  $\text{CDCl}_3$ ) 1.03 (3H, t,  $J$  7.2 Hz), 3.67–3.75 (1H, m), 3.80–3.88 (1H, m), 3.83 (1H, d, 17.1 Hz), 4.46 (1H, d, 17.1 Hz), 7.00–7.02 (2H, m), 7.14–7.18 (4H, m), 7.22–7.26 (2H, m), 7.43–7.45 (3H, m), 7.52–7.57 (4H, m);  $\delta_{\text{C}}$  (100 MHz,  $\text{CDCl}_3$ ) 13.6, 43.3, 61.5, 81.4 (q,  $J$  31 Hz), 98.5, 122.6 (q,  $J$  285 Hz), 126.7, 127.4, 127.7, 127.8, 128.1, 128.2, 129.05, 129.13, 129.6, 130.9, 138.0, 139.5, 165.3, 166.0.  $^{19}\text{F}$  NMR (376 MHz,  $\text{CDCl}_3$ )  $\delta_{\text{F}}$  -76.06. Anal. calcd for  $\text{C}_{26}\text{H}_{22}\text{F}_3\text{NO}_4$ : C, 66.52; H, 4.72; N, 2.98. Found: C, 66.42; H, 4.84; N, 3.14.

**5-Benzyl-3-methyl-2,2-diphenyl-5-(trifluoromethyl)oxazolidin-4-one (29d).** Colourless solid; m.p. 126–128 °C ( $\text{Et}_2\text{O}$ /hexane);  $\delta_{\text{H}}$  (300 MHz,  $\text{CDCl}_3$ ) 2.93 (3H, s), 3.22–3.32 (2H, m), 6.75–6.78 (2H, m), 6.99–7.02 (2H, m), 7.12–7.25 (5H, m), 7.32–7.41 (6H, m);  $\delta_{\text{C}}$  (75 MHz,  $\text{CDCl}_3$ ) 29.0, 37.0 (q,  $J$  1.2 Hz), 84.1 (q,  $J$  28.2 Hz), 98.9, 123.1 (q,  $J$  287 Hz), 127.2, 127.4, 127.46, 127.48, 128.0, 128.2, 128.3, 128.9, 129.0, 130.8, 133.0, 139.0, 140.2, 165.7. Anal. calcd for  $\text{C}_{24}\text{H}_{20}\text{F}_3\text{NO}_2$ : C, 70.06; H 4.90; N 3.40. Found: C, 69.97; H 4.91; N 3.37.

## Acknowledgements

We gratefully acknowledge the financial support from the Russian Science Foundation (Grant No. 16-13-10036). This research was carried out using resources of the Centre for Magnetic Resonance, the Computer Centre, and the Centre for Chemical Analysis and Materials of St. Petersburg State University.

## Notes and references

- (a) *1,3-Dipolar Cycloaddition Chemistry*, ed. A. Padwa, Wiley, New York, 1984; (b) *Synthetic Applications of 1,3-Dipolar Cycloaddition Chemistry Toward Heterocycles and Natural Products*, ed. A. Padwa and W. H. Pearson, John Wiley & Sons, New York, 2003; *Nitrile oxides, nitrones and nitronates in organic synthesis: novel strategies in synthesis*, ed. H. Feuer, John Wiley & Sons, Hoboken, 2008(c) A. G. Meyer and J. H. Ryan, *Molecules*, 2016, **21**, 935–988; (d) J. H. Ryan, *ARKIVOC*, 2015, (i), 160–183; (e) T. Hashimoto and K. Maruoka, *Chem. Rev.*, 2015, **115**, 5366–5412; (f) A. F. Khlebnikov and M. S. Novikov, *Chem. Heterocycl. Compd.*, 2012, **48**, 179–190.
- (a) R. Huisgen, *Angew. Chem., Int. Ed. Engl.*, 1963, **2**, 565–598; (b) R. Huisgen, *Angew. Chem., Int. Ed. Engl.*, 1963, **2**, 633–645.
- (a) *Pericyclic Reactions*, ed. A. P. Marchand and R. E. Lehr, Academic Press, New York, 1977, vol. I and II; (b) A. Williams, *Concerted organic and Bio-organic mechanisms*, CRC Press, Boca Raton, 2000.
- (a) G. Mlostoń, K. Urbaniak, M. Domagała, A. Pfitzner, M. Zabel and H. Heimgartner, *Helv. Chim. Acta*, 2009, **92**, 2631–2642; (b) A. F. Khlebnikov, A. S. Konev, A. A. Virtsev, D. S. Yufit, G. Mlostoń and H. Heimgartner, *Helv. Chim. Acta*, 2014, **97**, 453–470; (c) S. Emamian, *RSC Adv.*, 2016, **6**, 75299–75314.
- (a) *Fluorine in Heterocyclic Chemistry*, ed. V. Nenajdenko, Springer International Publishing, Switzerland, 2014, vol. 1; (b) P. He and S. Z. Zhu, *Mini-Rev. Org. Chem.*, 2004, **1**, 417–435.
- M. S. Novikov, A. F. Khlebnikov, M. V. Shevchenko, R. R. Kostikov and D. Vidovic, *Russ. J. Org. Chem.*, 2005, **41**, 1496–1506.
- M. S. Novikov, A. F. Khlebnikov, A. Krebs and R. R. Kostikov, *Eur. J. Org. Chem.*, 1998, 133–137.
- A. F. Khlebnikov, M. S. Novikov and R. R. Kostikov, *Mendeleev Commun.*, 1997, 127–128.
- C. Hansch, A. Leo and R. W. Taft, *Chem. Rev.*, 1991, **97**, 165–195.
- (a) N. S. Isaacs and O. H. Abed, *Tetrahedron Lett.*, 1986, **27**, 995–996; (b) L. Donxia, W. Dexian, L. Yaozhong and Z. Huaming, *Tetrahedron*, 1986, **42**, 4161–4167; (c) H. Yamataka, K. Nagareda, A. Ando and T. Hanafusa, *J. Org. Chem.*, 1992, **57**, 2865–2869; (d) H. Yamataka, K. Nagareda, T. Takatsuka, K. Ando, T. Hanafusa and S. Nagase, *J. Am. Chem. Soc.*, 1993, **115**, 8570–8576; (e) H. Yamataka, T. Takatsuka and T. Hanafusa, *J. Org. Chem.*, 1996, **61**, 722–726.
- Z.-K. Li, C. He, M. Yang, C.-Q. Xia and X.-Q. Yu, *ARKIVOC*, 2005, (i), 98–104.
- D. R. Edwards, P. Montoya-Peleaz and C. M. Crudden, *Org. Lett.*, 2007, **9**, 5481–5484.
- (a) A. D. Becke, *J. Chem. Phys.*, 1993, **98**, 5648–5652; (b) A. D. Becke, *Phys. Rev. A*, 1988, **38**, 3098–3100; (c) C. Lee,



- W. Yang and R. G. Parr, *Phys. Rev. B: Condens. Matter*, 1988, **37**, 785–789.
- 14 J. Tomasi, B. Mennucci and R. Cammi, *Chem. Rev.*, 2005, **105**, 2999–3093.
- 15 J.-D. Chai and M. Head-Gordon, *Phys. Chem. Chem. Phys.*, 2008, **10**, 6615–6620.
- 16 Y. Zhao and D. G. Truhlar, *J. Phys. Chem. A*, 2004, **108**, 6908–6918.
- 17 M. Ríos-Gutiérrez, A. Darù, T. Tejero, L. R. Domingo and P. Merino, *Org. Biomol. Chem.*, 2017, **15**, 1618–1627.
- 18 (a) J. Wang, M. Sanchez-Rosello, J. L. Acena, C. del Pozo, A. E. Sorochinsky, S. V. Fustero, V. A. Soloshonok and H. Liu, *Chem. Rev.*, 2014, **114**, 2432–2506; (b) *Fluorine in Heterocyclic Chemistry*, ed. V. Nenajdenko, Springer Verlag, Berlin, 2013, vol. 1 and 2; (c) *Fluorinated Heterocyclic Compounds*, ed. V. A. Petrov, J. Wiley & Sons Inc., Hoboken, 2009.
- 19 (a) J. A. Young, T. C. Simmons and F. W. Hoffmann, *J. Am. Chem. Soc.*, 1956, **78**, 5637–5639; (b) T. Abe, E. Hayashi, H. Baba and H. Fukaya, *J. Fluorine Chem.*, 1990, **48**, 257–279.
- 20 (a) M. S. Novikov, I. V. Voznyi, A. F. Khlebnikov, J. Kopf and R. R. Kostikov, *J. Chem. Soc., Perkin Trans. 1*, 2002, 1628–1630; (b) I. V. Voznyi, M. S. Novikov, A. F. Khlebnikov, J. Kopf and R. R. Kostikov, *Russ. J. Org. Chem.*, 2004, **40**, 199–205; (c) I. V. Voznyi, M. S. Novikov, A. F. Khlebnikov and R. R. Kostikov, *Russ. Chem. Bull.*, 2004, **53**, 1087–1091.
- 21 M. J. Frisch, G. W. Trucks, H. B. Schlegel, G. E. Scuseria, M. A. Robb, J. R. Cheeseman, G. Scalmani, V. Barone, B. Mennucci, G. A. Petersson, H. Nakatsuji, M. Caricato, X. Li, H. P. Hratchian, A. F. Izmaylov, J. Bloino, G. Zheng, J. L. Sonnenberg, M. Hada, M. Ehara, K. Toyota, R. Fukuda, J. Hasegawa, M. Ishida, T. Nakajima, Y. Honda, O. Kitao, H. Nakai, T. Vreven, J. A. Montgomery Jr., J. E. Peralta, F. Ogliaro, M. Bearpark, J. J. Heyd, E. Brothers, K. N. Kudin, V. N. Staroverov, T. Keith, R. Kobayashi, J. Normand, K. Raghavachari, A. Rendell, J. C. Burant, S. S. Iyengar, J. Tomasi, M. Cossi, N. Rega, J. M. Millam, M. Klene, J. E. Knox, J. B. Cross, V. Bakken, C. Adamo, J. Jaramillo, R. Gomperts, R. E. Stratmann, O. Yazyev, A. J. Austin, R. Cammi, C. Pomelli, J. W. Ochterski, R. L. Martin, K. Morokuma, V. G. Zakrzewski, G. A. Voth, P. Salvador, J. J. Dannenberg, S. Dapprich, A. D. Daniels, O. Farkas, J. B. Foresman, J. V. Ortiz, J. Cioslowski and D. J. Fox, *Gaussian 09, Revision D.01*, Gaussian, Inc., Wallingford CT, 2013.

